Available online at www.sciencedirect.com

Dyes and Pigments 77 (2008) 673–677

www.elsevier.com/locate/dyepig

Synthesis and analysis of UV/visible spectra of carbocyanine dimer models

Masaru Kimura*, Takeshi Fukai, Tomoyuki Kinoshita

Department of Chemistry, Faculty of Science, Graduate School of Natural Science and Technology, Okayama University,
Tsushimanaka 3-1-1, Okayama 700-8530, Japan

Received 12 December 2006; received in revised form 19 January 2007; accepted 20 January 2007
Available online 8 April 2007

Abstract

Dimers **1** and **2**, having a pair of the carbocyanine moieties connected at the *meso*-positions by an —O—Ph—O— or —S—Ph—S— bridge, were prepared. Their UV/visible spectra displayed a first absorption maxima at ca. 750 nm, a second absorption maxima at ca. 800 nm and a shoulder at ca. 850 nm. Since MOPAC calculations indicated that the configuration of the dimers was folded, but twisted, strong H-type coupling together with weaker J-type coupling takes place along the longer axis of the dimers. The UV/visible spectra of the dimers were characterized by a split in the long wavelength absorption of the corresponding carbocyanine chromophore into a more intense blue shift and a less intense red shift. Remarkably, the dimers showed greater sensitivity to solvent polarity than the monomers **3** and **4**.
© 2007 Published by Elsevier Ltd.

Keywords: Carbocyanine dye; *meso*-Substituted cyanine; Intramolecular charge transfer; J-coupling; H-coupling

1. Introduction

Cyanine dyes as photo-sensitizers have been widely used for image recording processes such as photography and photo-polymerization [1–4]. It is well known that the interactions between cyanine dyes provide unique properties related to H-type and J-type aggregation. As the most simplified aggregation model is dimeric, research into cyanine dye aggregation has focused on the use of dimers as models [5,6]. In this context, this paper concerns with new dimer models of a carbocyanine dye, which consist of two carbocyanine moieties linked by an —S—Ph—S— or —O—Ph—O— bridge (Fig. 1), as a means of examining the interactions between the two dye moieties. MOPAC calculations were performed to estimate the extent of overlapping using ∠C—S—C and ∠C—O—C bond angles, the lengths of the bridges, and the distances between the dye moieties. Solvatochromic behaviour was assessed by changing solvent polarity using methanol, acetone, acetonitrile (CH_3CN), chloroform, *N*,*N*-dimethyl-formamide (DMF), and dimethylsulfoxide (DMSO).

The nature of the excitonic interactions is discussed in terms of UV/visible spectroscopic analysis and the MOPAC calculations.

2. Results and discussion

2.1. UV/visible absorption and solvatochromic effect

The carbocyanine dyes are generally anticipated to have a π,π* transition with weak charge-transfer character in the ground state but considerably stronger charge separation in the excited state, as well as a consequent positive solvatochromic effect [8]. The transition energies of several carbocyanine dyes show reasonable quantitative correlations with the typical empirical solvent polarity parameter, the Kamlet—Taft π^* parameter, which is a measure of the polarity/polarizability effect of the solvent [7,9]. The Kamlet—Taft treatment is attractive as it allows the separation of "polarity" from other

---

* Corresponding author. Tel./fax: +81 86 251 7839.
E-mail address: kimuram@cc.okayama-u.ac.jp (M. Kimura).

0143-7208/$ - see front matter © 2007 Published by Elsevier Ltd.
doi:10.1016/j.dyepig.2007.01.025

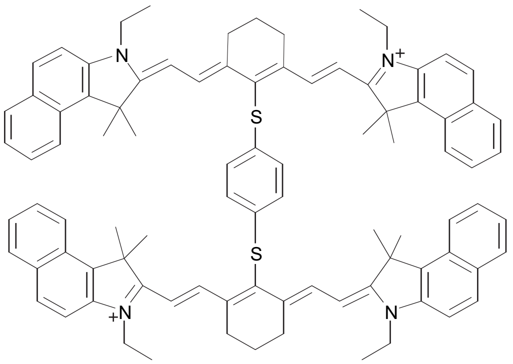

$2BF_4^-$

1

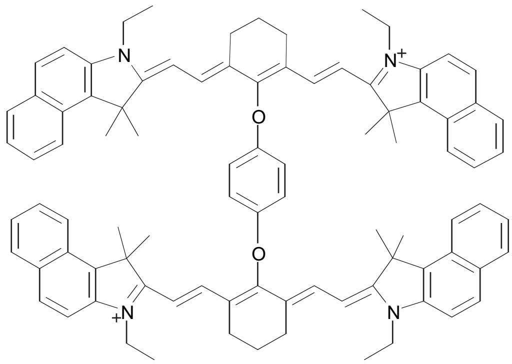

$2BF_4^-$

2

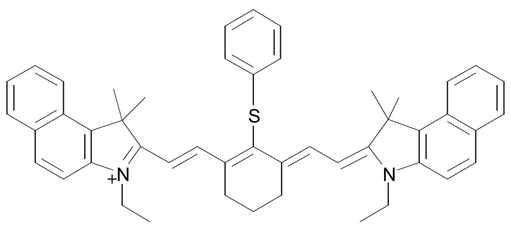

BF_4^-

3

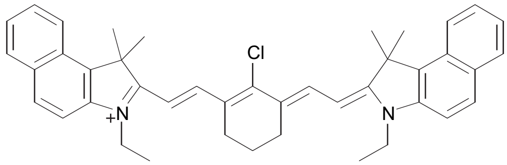

BF_4^-

4

Fig. 1. Dimers **1** and **2**, and monomer models **3** and **4**.

solvent–solute interactions, such as hydrogen bonding. The transition energies of the monomers **3** and **4** in various solvents are summarized in Table 1. A plot of transition energy versus the empirical solvent π^* gives a linear plot of negative slope ($-s$) in the case where there is more charge separation in the excited state than in the ground state. When the absorption maxima of monomers **3** and **4** are plotted versus π^*, reasonable linear plots are obtained by fitting Eqs. (1) and (2) using least-squares method:

$$E_{\max}(\mathbf{3}) = 35.6\,\mathrm{kcal} - 1.72\pi^* \quad (1)$$

$$R = 0.88,\ N = 6$$

Table 1
Absorption maxima of monomer models **3** and **4**

Solvent	Taft π^*	Monomer **3** $\lambda_{\max}$		Monomer **4** $\lambda_{\max}$	
		nm	kcal/mol	nm	kcal/mol
Methanol	0.586	827 755	34.571 37.868	816 748	35.037 38.222
Acetone	0.683	830 757	34.446 37.768	818 749	34.951 38.171
CH_3CN	0.713	827 748	34.571 38.222	815 749	35.080 38.171
Chloroform	0.760	839 764	34.076 37.421	826 752	34.613 38.019
DMF	0.875	838 764	34.117 37.421	826 755	34.613 37.868
DMSO	1.000	843 770	33.915 37.130	831 762	34.404 37.520

$$E_{\max}(\mathbf{4}) = 36.1\,\mathrm{kcal} - 1.67\pi^* \quad (2)$$

$$R = 0.89,\ N = 6$$

2.2. Exciton coupling

Dimers **1** and **2** comprise a pair of carbocyanines connected at the *meso*-positions by the –S–Ph–S– and –O–Ph–O– bridge, respectively. Table 2 shows the first absorption maxima at ca. 750 nm, the second absorption maxima at ca. 800 nm and a shoulder at ca. 850 nm for dimers **1** and **2** (Fig. 3), which were independent of concentration over the range 10^{-5}–10^{-7} M. When the solvent was changed from methanol, to acetone, to CH_3CN, to chloroform, to DMF and then to DMSO, all absorption maxima underwent a modest red shift (Table 2).

The spectral shapes for dimers **1** and **2** are basically identical, while all three peaks for the dimer **1** were located at longer wavelengths than those for the dimer **2**. For all solvents employed, the dominant band was located at shorter wavelength (~750 nm) with a high ε, middle medium peak at ca. 800 nm which can be attributed to that of the corresponding carbocyanine moieties and the longer wavelength (~850 nm) with a low ε. For tethered squaraines, the short-wavelength band was attributed to a folded H-type dimer [6]. The appearance of the short-wavelength band is common for the H-aggregates of carbocyanine dyes. The strong, shorter wavelength absorption (ε: 400,000–200,000) for dimers **1** and **2** implies that intramolecular H-type excitonic interaction is very strong and

Table 2
Absorption maxima of dimers **1** and **2**

Solvent	Taft π*	Dimer **1** λ_{max}		Dimer **2** λ_{max}	
		nm	kcal/mol	nm	kcal/mol
Methanol	0.586	752 807 865	38.019 35.428 33.052	730 789	39.164 36.236
Acetone	0.683	756 808 856	37.817 35.384 33.400	735 788	38.898 36.282
CH_3CN	0.713	752 803 855	38.019 35.604 33.439	732 787	39.057 36.328
Chloroform	0.760	761 812 860	37.569 35.209 33.244	740 794	38.635 36.008
DMF	0.875	764 816 861	37.421 35.037 33.206	743 793	38.479 36.053
DMSO	1.000	768 820 867	37.227 34.866 32.976	746 797	38.324 35.872

that the chromophores overlap very well. The structures of dimers **1** and **2**, in their lowest energy configurations obtained by MOPAC calculation, are shown in Fig. 2. The slid configuration should give rise to small J-type excitonic coupling, characterized by a split in π,π* transition leading to lower energy (less allowed) and higher energy (more allowed) transitions compared to those of the monomers.

Based on MOPAC calculations, the bridge length for dimer **1** was 8.189 Å larger than the value of 7.286 Å for dimer **2**, although the extent of the twist for dimer **1** is a little more than that for dimer **2**. The difference in the extent of the twist is probably reflected by the difference in extinction coefficients at ca. 850 nm, as shown in Fig. 3.

The absorption energies for the first absorption band were plotted against the π* values (Table 2), and this plot gives a good fit.

$$E_{\max}(\text{dimer }\mathbf{1}) = 39.2\,\text{kcal} - 2.08\pi^* \tag{3}$$

$$R = 0.93,\ N = 6$$

$$E_{\max}(\text{dimer }\mathbf{2}) = 40.5\,\text{kcal} - 2.18\pi^* \tag{4}$$

$$R = 0.95,\ N = 6$$

The absorption energies for the second absorption band were plotted against the π* values (Table 2), and this plot gives a fair fit.

$$E_{\max}(\text{dimer }\mathbf{1}) = 36.5\,\text{kcal} - 1.62\pi^* \tag{5}$$

$$R = 0.87,\ N = 6$$

$$E_{\max}(\text{dimer }\mathbf{2}) = 36.9\,\text{kcal} - 1.01\pi^* \tag{6}$$

$$R = 0.83,\ N = 6$$

The values of the slopes ($s = -1.01$ to -1.62) for the second absorption and those of the monomers ($s = -1.67$ to 1.72) were rather small, compared to the values ($s = -2.08$ to -2.18) for the first absorption corresponding to H-type coupling. Stronger H-type coupling and a less effective J-type coupling are expected from a slightly twisted configuration along the longer axis of the dimers (Fig. 2). The UV/visible spectra of the dimers are characterized by more intense blue shifted and less intense red shifted absorptions. Remarkably, the dimer model shows a greater sensitivity to solvent polarity than the monomer model.

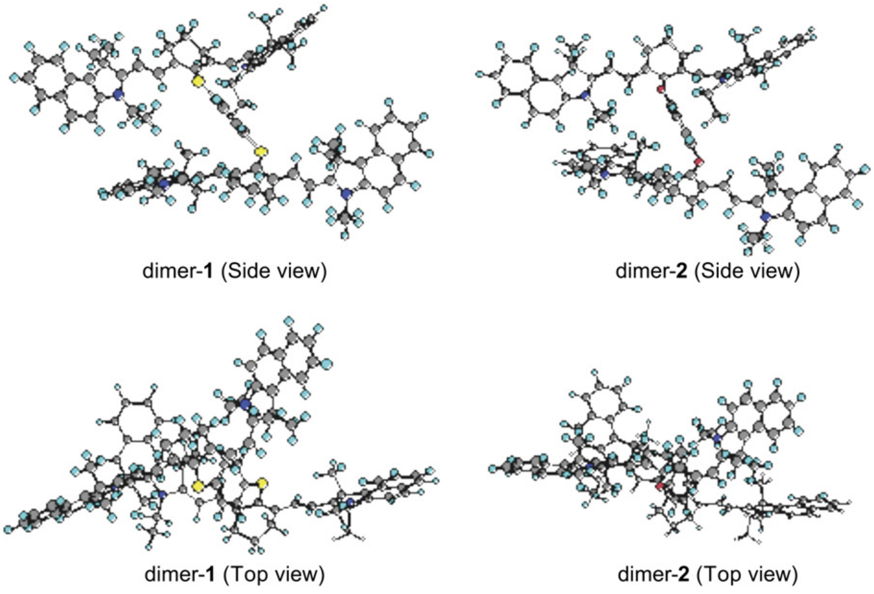

Fig. 2. Optimized structures (MOPAC AM1) of the dimers **1** and **2**.

3. Conclusions

The excitonic interactions of cyanine dyes have been investigated by comparing the UV/visible absorption spectra of the dimer models **1** and **2** and the monomer models **3** and **4**. The UV/visible spectra for the dimers have three peaks, a first absorption maxima at ca. 750 nm, a second at ca. 800 nm and a shoulder at ca. 850 nm due to interactions, while the monomers **3** and **4** have absorption maxima at ca. 800 nm and a shoulder at ca. 750 nm (Fig. 3). Due to the low solubility of dimers **1** and **2**, it was possible to only use solvents having Kamlet–Taft π^* values >0.586 [7]. Remarkably, the dimer showed greater sensitivity to solvent polarity than the corresponding monomer.

MOPAC calculations indicated that the configuration of the dimers was nearly folded but twisted slightly, it is reasonable to propose that strong H-type coupling and less effective J-type coupling occur along the longer axis of the dimers. The UV/visible spectra of the dimers were characterized by a split in the long wavelength absorption of the corresponding carbocyanine chromophore into a more intense blue shift and a less intense red shift. Remarkably, the dimers **1** and **2** showed greater solvatochromic sensitivities, s values of which were -2.08 and -2.18, respectively, than the monomer models **3** and **4** ($s = -1.72$ and -1.67).

4. Experimental

4.1. General

Melting points were determined with a Yanagimoto micro melting point apparatus and are uncorrected. Infrared (IR) spectra were recorded on a JASCO FT/IR-5000 spectrometer while UV/visible spectra were measured using a HITACHI UV-288 spectrophotometer and JASCO V-530 UV/visible spectrophotometer. The NMR spectra were measured on a Varian Unity INOVA AS600 (600 MHz), VXR500 (500 MHz). Elemental analysis was performed by a Yanagimoto C.H.N. recorder MI-2 type.

The solvents used for UV/visible measurement, which were all of spectral grade, were purchased from Nakarai Tesque Inc. (Tokyo, Japan). Sensitizing dye **4** was purchased from Hayashibara Biochemical Laboratories.

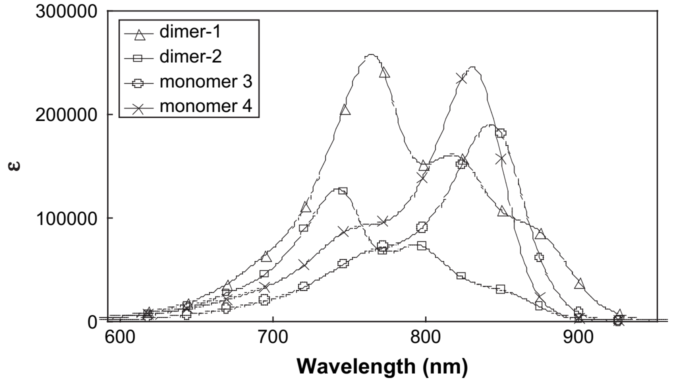

Fig. 3. UV/visible absorption spectra of dimers **1** and **2**, and monomer models **3** and **4** in DMSO.

4.1.1. Preparation of meso-substituted carbocyanine dimer *1*

A mixture of 1,4-benzenethiol (54 mg, 0.38 mmol) and **4** (497 mg, 0.71 mmol) in distilled DMF was stirred under a nitrogen atmosphere at room temperature. The mixture was poured into 500 ml of water and the dimer **1** was obtained as deep, golden red prisms in 70% yield (363 mg, 0.25 mmol). ^{1}H NMR (600 MHz, acetone-d_6) δ 1.27 (t, $J = 7.2$ Hz, 12H), 1.69 (br s, 24H), 1.96 (quin, $J = 6.0$ Hz, 4H), 2.77 (t, $J = 6.0$ Hz, 8H), 4.24 (q, $J = 7.2$ Hz, 8H), 6.35 (d, $J = 14.4$ Hz, 4H), 7.40–7.43 (m, 8H), 7.45 (t, $J = 8.4$ Hz, 4H), 7.54 (d, $J = 9.0$ Hz, 4H), 7.93 (t, $J = 9.0$ Hz, 8H), 8.04 (d, $J = 9.0$ Hz, 4H), 8.32 (d, $J = 13.8$ Hz, 4H). IR (KBr) 2926, 1352, 1236, 1060, 965, 878 cm^{-1}. Anal. calcd for $C_{90}H_{92}B_2F_8N_4S_2 \cdot 3H_2O$: C, 71.05; H, 6.49; N, 3.68. Found: C, 71.17; H, 6.43; N, 3.70.

4.1.2. Preparation of meso-substituted carbocyanine dimer *2*

A solution of hydroquinone (44.8 mg, 0.41 mmol) in anhydrous chloroform/distilled methanol (4:1, v:v), stirred under a nitrogen atmosphere at room temperature until evolution of hydrogen ceased (10 min), was treated with a solution of **4** (501 mg, 0.72 mmol) in anhydrous chloroform. After stirring for 10 h at room temperature the mixture was poured onto dry-ice and concentrated on a rotary evaporator. Chromatography on silica gel with chloroform/methanol as eluent (gradient, up to 20% of methanol) was followed by crystallization from MeOH/Et_2O. The dimer **2** was obtained as deep green powder in a 17% yield (80 mg, 0.06 mmol). ^{1}H NMR (600 MHz, acetone-d_6) δ 1.17 (t, $J = 7.2$ Hz, 12H), 1.72 (s, 24H), 1.94 (quin, $J = 2.4$ Hz, 4H), 2.76 (t, $J = 7.2$ Hz, 8H), 4.18 (q, $J = 7.2$ Hz, 8H), 6.23 (d, $J = 14.4$ Hz, 4H), 7.29 (t, $J = 8.4$ Hz, 4H), 7.37–7.40 (m, 8H), 7.53 (d, $J = 8.4$ Hz, 4H), 7.99 (d, $J = 9.0$ Hz, 12H), 8.13 (d, $J = 14.4$ Hz, 4H). IR (KBr) 2926, 1352, 1232, 1093, 1058, 963, 801 cm^{-1}. HRMS-FAB: calcd for $C_{90}H_{92}B_2F_8N_4O_2^{2+}$: 1260.7220; found: 1260.7217.

4.1.3. Preparation of meso-substituted carbocyanine monomer *3*

A mixture of **4** (200 mg, 0.29 mmol) and benzenethiol (35 mg, 0.32 mmol) in DMF was stirred at room temperature under a nitrogen atmosphere for 12 h. The solution was poured into water and the aqueous mixture was extracted with five 100 ml portions of chloroform. The organic layer was dried with anhydrous magnesium sulfate and the chloroform was evaporated. The residue was purified on a silica gel column with chloroform/methanol solution as eluent. Monomer **3** was obtained as a cyan powder in 38% yield (84.3 mg, 0.11 mmol). ^{1}H NMR (600 MHz, acetone-d_6) δ 1.48 (t, $J = 7.2$ Hz, 6H), 1.77 (br s, 12H), 2.08 (quin, $J = 6.0$ Hz, 2H), 2.79 (t, $J = 6.0$ Hz, 4H), 4.25 (q, $J = 7.2$ Hz, 4H), 6.35 (d, $J = 14.4$ Hz, 2H), 7.09 (quin, $J = 3.0$ Hz, 1H), 7.26–7.29 (m, 4H), 7.39 (d, $J = 8.4$ Hz, 2H), 7.45 (t, $J = 7.2$ Hz, 2H), 7.56 (t, $J = 7.2$ Hz, 2H), 8.04 (d, $J = 8.4$ Hz, 4H), 8.04 (d, $J = 8.4$ Hz, 2H), 8.80 (d, $J = 14.4$ Hz, 2H). IR (KBr) 2926, 1388, 1352, 1058, 963 cm^{-1}. Anal. calcd for $C_{48}H_{49}N_2S_1 \cdot 5/3BF_4$: C, 69.40; H, 5.95; N, 3.37. Found: C, 69.49; H, 5.98; N, 3.43.

Acknowledgements

The Ministry of Education, Science, Sports and Culture of Japan financially supported this work by a Science Research Grant-in-Aid (15550037, 17029042). We also thank the SC-NMR Laboratory of Okayama University for the measurements of ^1H NMR spectra.

Appendix. Supplementary data

Supplementary data associated with this article can be found in the online version, at doi:10.1016/j.dyepig.2007.01.025.

References

[1] Monroe BM, Weed GC. Photoinitiators for free-radical-initiated photoimaging systems. Chem Rev 1993;93:435–48.

[2] Murphy S, Yang X, Schuster GB. Cyanine borate salts that form penetrated ion pairs in benzene solution: synthesis, properties, and structure. J Org Chem 1995;60:2411–22.

[3] Kimura M, Mitekura H, Fujie T, No T. Development of new three component photo-polymerization systems even efficient near the infrared region. Bull Chem Soc Jpn 2002;75:1159–62.

[4] Kimura M, Mitekura H, No T, Suzuki K. Synthesis of *meso*-substituted trimethine cyanine dyes and evaluation of their sensitivities in sensitized photo-polymerization. Bull Chem Soc Jpn 2002;75:2655–60.

[5] Tu B, Ghosh B, Lightner DA. A new class of linear tetrapyrroles: acetylenic 10,10a-dihydro-10a-homobilirubins. J Org Chem 2003;68:8950–9863.

[6] Lu L, Lachicotte RJ, Penner TL, Perlstein J, Whitten DG. Exciton and charge-transfer interaction in nonconjugated merocyanine dye dimer: novel solvatochromic behavior for tethered bichromophores and eximers. J Am Chem Soc 1999;121:8146–56.

[7] Kamlet MJ, Abboud JL, Taft RW. J Am Chem Soc 1977;99:6027–38.

[8] Mitekura H, Suzuki K, No T, Satake K, Kimura M. Spectroscopic properties of *meso*-substituted cyanine dyes: evidences for intramolecular charge transfer from a julolidine moiety as a *meso*-substituent to the cyanine chromophore. Dyes Pigments 2002;113–20.

[9] Brooker LGS, Craig AC, Heseltine DW, Jenkins PW, Lincoln L. Color and constitution. XIII. Merocyanines as solvent property indicators. J Am Chem Soc 1965;87:2443–50.